

GA-A22872

**SCALING AND PROFILES OF HEAT FLUX
DURING PARTIAL DETACHMENT IN DIII-D**

by

**C.J. LASNIER, D.N. HILL, S.L. ALLEN, M.E. FENSTERMACHER,
A.W. LEONARD, T.W. PETRIE, G.D. PORTER, and J.G. WATKINS**

AUGUST 1998

DISCLAIMER

This report was prepared as an account of work sponsored by an agency of the United States Government. Neither the United States Government nor any agency thereof, nor any of their employees, makes any warranty, express or implied, or assumes any legal liability or responsibility for the accuracy, completeness, or usefulness of any information, apparatus, product, or process disclosed, or represents that its use would not infringe privately owned rights. Reference herein to any specific commercial product, process, or service by trade name, trademark, manufacturer, or otherwise, does not necessarily constitute or imply its endorsement, recommendation, or favoring by the United States Government or any agency thereof. The views and opinions of authors expressed herein do not necessarily state or reflect those of the United States Government or any agency thereof.

SCALING AND PROFILES OF HEAT FLUX DURING PARTIAL DETACHMENT IN DIII-D

by

C.J. LASNIER,[†] D.N. HILL,[†] S.L. ALLEN,[†] M.E. FENSTERMACHER,[†]
A.W. LEONARD, T.W. PETRIE, G.D. PORTER,[†] and J.G. WATKINS[‡]

This is a preprint of a paper to be presented at the 13th International Conference on Plasma Surface Interactions on Controlled Fusion Devices, May 18–23, 1998, San Diego, California and to be published in *Journal of Nuclear Materials*.

[†]Lawrence Livermore National Laboratory

[‡]Sandia National Laboratories, Albuquerque

Work supported by
the U.S. Department of Energy
under Contracts DE-AC03-89ER51114, DE-AC04-94-AL85000,
and W-7405-ENG-48

GA PROJECT 3466
AUGUST 1998

ABSTRACT

We examine the scaling of the peak divertor heat flux and total divertor plate power in partially detached divertor (PDD) discharges in DIII-D, as a function of input power and radiated power. The peak divertor heat flux in the attached plasma increases linearly with input power, but saturates in the detached cases. The total divertor plate power remains linear with input power in both the attached and detached plasmas. This is consistent with the fact that the heat flux peak is reduced from the attached case but other areas receive increased radiant heating from the detached plasma. The divertor plate radiant heating is linear with input power because the total radiated power from the entire plasma is a linear function of input power in both attached and detached plasma. In the private flux region, radiated heat flux absorbed on the target plate calculated from bolometer data is enough to account for the measured plate heating. Approximately half of the overall plate heating power in detached plasma is due to absorbed radiation. By mapping the divertor heat flux before and during the PDD to flux coordinates, and comparing with a flux mapping of inverted bolometer and tangential TV data, we have verified that the radiated power is emitted from the same flux surfaces on which heat flux is reduced.

1. INTRODUCTION

Moderating the peak heat flux \hat{q} is a major concern in tokamak divertor design, and the reference operating point for ITER requires a factor of 5 reduction in \hat{q} . However, little is known about how the peak heat flux and radial divertor heat flux profile shape $q(R)$ vary with either input power or radiation fraction. We have observed a factor of 3-5 reduction in \hat{q} at 10 MW input power in DIII-D, and in this paper we will examine the scaling of \hat{q} and divertor plate power with input power. Because electron conduction cannot be the dominant energy transport mechanism [1] in the low-temperature PDD regime [2] as it is in the attached state, we might expect \hat{q} scaling with input power to differ from the attached case in which \hat{q} varies linearly with input power [3,4].

In the DIII-D open divertor, deuterium gas puffing from either the private flux region or the plasma midplane produces a PDD condition which can reduce \hat{q} by a factor of 5, while total radiated power (the integral over the entire plasma) increases by only a factor of 1.7. We examine the effect of the resulting 2-D radiation profile on the divertor heat flux profile shape. The total radiative heating power absorbed at the plate, calculated from bolometer data, is compared with the total measured power deposited on the plate. After comparing $q(R)$ and the calculated profile of radiated heating on the plate, we attribute the difference to particle interaction with the plate.

We focus here on data from lower single-null (LSN) discharges at the outer strike point. A set of DIII-D discharges was chosen having D₂ puffing and a range of neutral beam injected power levels from 2.5 to 14 MW. The density varied from $4 \times 10^{19} \text{ m}^{-3}$ before puffing to $8 \times 10^{19} \text{ m}^{-3}$ after puffing. We take the neutral beam injected power P_{inj} as a good approximation of the input power as the beam power is completely absorbed in DIII-D at these densities. Ohmic power was less than 0.35 MW and will not be included. The discharges at the time of the measurements were nearly steady-state so the stored energy w was changing slowly, and dw/dt was typically 10% of the input power or less. Energy confinement decreased by less than 10% after gas puffing in many of these discharges, although a few showed a larger decrease. Plasma current was either 1.0 or 1.3 MA, with toroidal field of 2.1 T.

We measure the divertor heat flux in DIII-D using infrared thermography. The heat flux is averaged over ELMs by the thermal inertia of the divertor plates [4], with an estimated margin of error which is the greater of 15% of the measured value or 0.1 MW/m². All divertor plate peak heat flux data is for the outer strike point. Values for total power on the divertor plate represent integrals over the entire $q(R)$ profile, and toroidal symmetry is assumed.

2. EXPERIMENT

2.1 DIVERTOR HEAT FLUX VERSUS INPUT POWER

We find \hat{q} is linear over our whole range of power for the attached plasma, but the detached \hat{q} appears to be saturating at near 1.2 MW/m^2 as P_{inj} increases, as seen in Fig. 1(a). The linear dependence of the attached \hat{q} on P_{inj} is consistent with previous findings [4]. In contrast, the total plate power varies linearly with P_{inj} as shown in Fig. 1(b), in both the attached and detached cases. This difference between the peak and integrated heat flux behavior is due to the reduction of the heat flux peak and broad increase in absorbed radiation at the divertor plate. It is uncertain how this saturation of the detached peak heat flux will extrapolate to higher power or larger machines. If a similar effect carries over to reactors, this is quite a beneficial result.

2.2. RADIATED POWER

Total radiated power was calculated by integrating over a 2-D profile obtained by inverting bolometer data [5,6] and assuming toroidal symmetry, and was found to increase linearly with the input power in both the detached and attached phases. In Fig. 2 is shown the variation of radiated power (P_{rad}) with input power for (a) detached plasma, and (b) attached plasma. Radiated power from below the X-point in the outer divertor and outer SOL above the X-point were also integrated separately and shown in Fig. 2. The radiation from each of the regions was at least roughly linear with increasing P_{inj} for both attached and detached plasma. Power radiated from inside the separatrix is similar to that from the outer divertor. The core radiation fraction was approximately constant.

2.3. RADIATED FRACTION

The radiated power fraction for these discharges was calculated by dividing total radiated power by injected power P_{inj} . The radiated fraction in the attached and detached (post-puff) state are plotted in Fig. 3 against P_{inj} . There is some variability in the detached data at low power, but the discharges at intermediate and highest powers show a radiated fraction near 0.7. In the attached plasmas the radiated fraction ranges from 0.35 to 0.55. The fact that radiated power fraction did not decrease in the detached plasmas at high input power is at least partly due to the extra gas puffing supplied to the plasma. The puff rate was not intentionally adjusted to give fixed radiated fraction, but rather to obtain similar divertor plasma conditions.

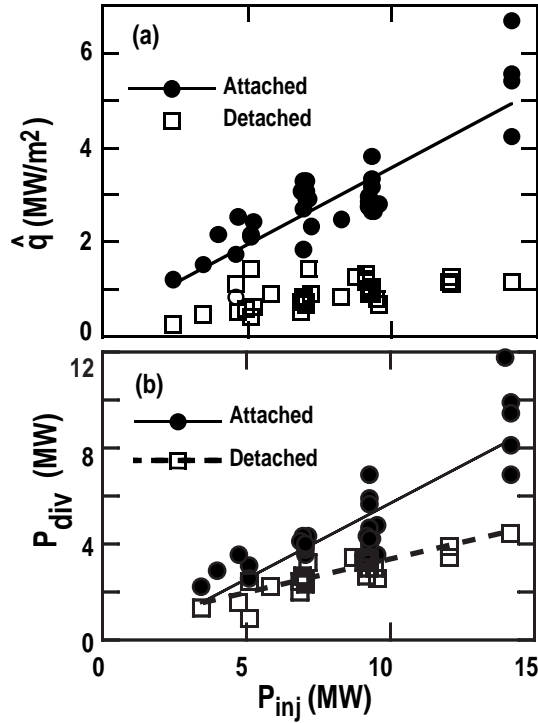


Fig. 1. (a) Experimentally measured peak heat flux versus injected power for attached and detached plasma. For these plots the detached heat flux and divertor power were smoothed over a 0.5 s time window before the values were extracted for each discharge. This was done because of the low thermal radiation signal from the plate in the detached state. (b) Total divertor plate power versus injected power, attached and detached.

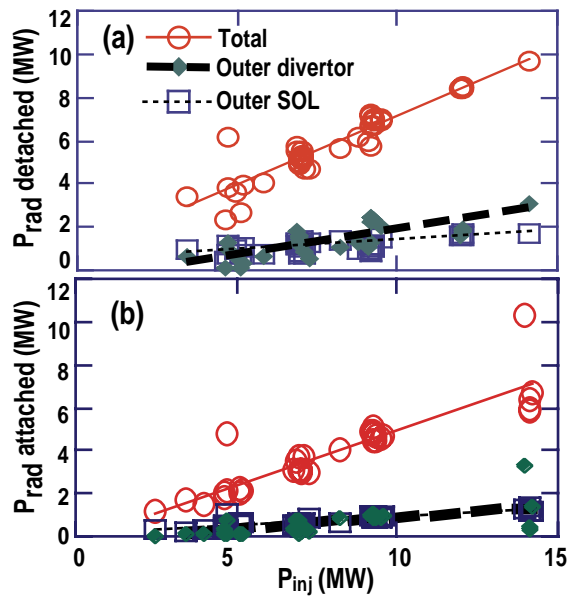


Fig. 2. Radiated power versus injected power for various regions for (a) detached and (b) attached plasma. Here the SOL is above the X-point outside the separatrix, and the outer divertor is below the X-point outside the separatrix. All lines through experimental data in this and succeeding figures are least squares fits to the data.

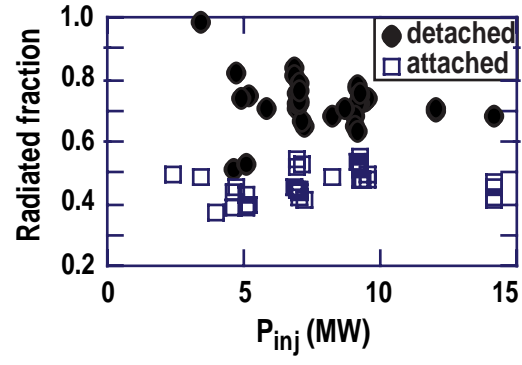


Fig. 3. Fraction of injected power radiated versus injected power from DIII-D data.

2.4. RADIANT HEATING OF DIVERTOR PLATE

The profile of radiant heat flux absorbed on the divertor plate was calculated from the 2-D distribution of plasma radiation, obtained from bolometer inversions. The calculation was done for each point on the divertor plate by integrating over the spatial distribution of radiation found in the bolometer inversion. This is similar to analysis previously done by Leonard for attached plasma [5]. We assume all of the incident radiation was absorbed in the plate, which is reasonable because the radiated power is largely ultraviolet.

Figure 4 shows the plate heat flux profile measured by thermography, and the calculated heat profile produced on the plate by absorbed plasma radiation, for a detached plasma. We see that the radiant heating is sufficient to account for all the heat flux in the private flux region and at the outer separatrix in a detached plasma. This indicates that no significant fraction of the heat is carried to the plate by particles in those areas. In the outer leg away from the separatrix, particle flux is still important.

In Fig. 5(a) the peak radiant heat flux on the plate for detached plasma is plotted against P_{inj} and is seen to be linear over the whole range of power, as is the total radiant power onto the divertor plate in Fig. 5(b). This is consistent with the finding above that the radiated power is linear with P_{inj} .

The fact that both the calculated radiant heating of the divertor plate and the measured plate heating are linear with input power may imply that increased optical depth of divertor plasma is not playing a role as we puff more gas at higher power. Re-absorption of radiation by the plasma is not included in the radiant heating calculation.

In Fig. 5(c) we show the total power on the divertor plate from infrared thermography, plotted against the radiant plate heating power. From the slope of the fitted line we see that on

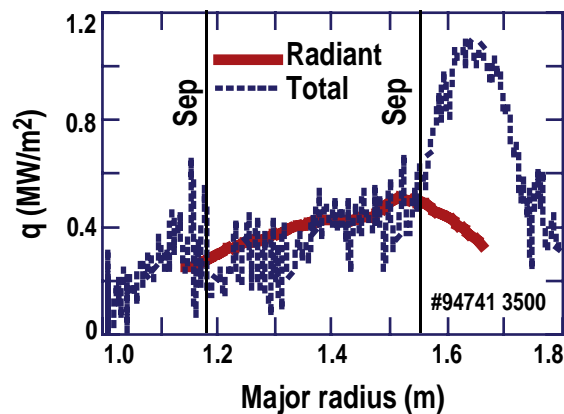


Fig. 4. Divertor heat flux profile for a detached plasma. The dashed curve is the total heat flux measured by IR thermography. The solid curve is the radiant heat flux calculated from bolometer radiation data. The label “Sep” signifies the separatrix location at the plate.

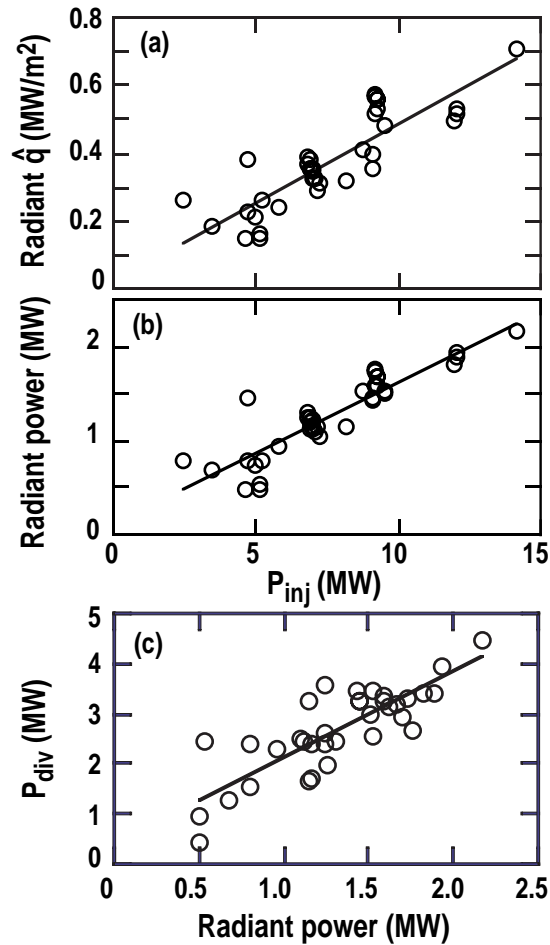
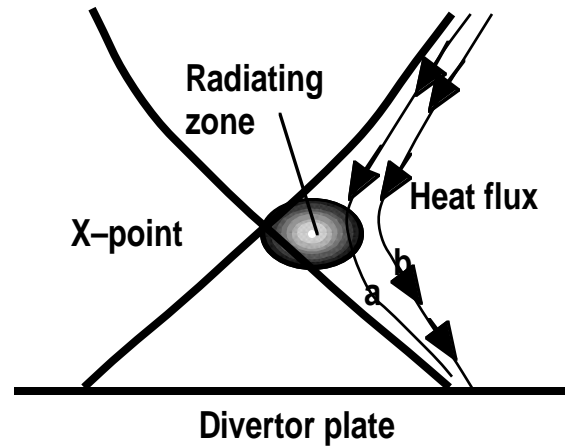


Fig. 5. (a) Peak radiant heat flux absorbed on the divertor plate versus injected power; (b) Total radiant power absorbed on the divertor plate versus injected power; (c) Total divertor plate power measured by IR camera during detachment versus radiant power absorbed on the plate calculated from bolometers.

average, half of the plate heating power in detached plasma is due to absorbed radiation. The half of the plate power not due to radiant heating is caused by interaction of particles with the plate. This includes heat flux conducted and convected to the plate by ions, as well as heat deposited by neutrals generated by recombination, and any charge exchange flux. A significant part of the heat in detached operation is deposited by ELMs [7].

2.5. COMPARISON OF FLUX SURFACE DISTRIBUTION OF SOL RADIATION WITH FLUX SURFACE PROFILE OF DIVERTOR HEAT REDUCTION

We find that the field lines which conduct the most heat to the plate in the attached case are the same field lines on which strong radiation is emitted in the detached case, which is depicted schematically in Fig. 6. This is in agreement with behavior expected from conservation of energy



*Fig. 6. Reduction of divertor plate heat flux by a radiating zone. Heat is depicted flowing along flux surfaces *a* and *b* toward the plate. The heat on surface *a* is intercepted by a radiating zone, while the heat on surface *b* travels relatively undiminished to the plate.*

and strong conduction of heat along field lines upstream of the radiating zone. To compare the flux surface distribution of heat and radiation, we mapped the heat flux profiles and radiation profiles to normalized poloidal flux coordinates.

The emission measured by bolometers and inverted into a 2-D profile was mapped to coordinates of normalized poloidal flux and poloidal length to the divertor plate (L_{pol}) along a flux surface. In these coordinates, all radiation emitted on a vertical line is radiated from the same flux surface, which can be compared directly with the divertor heat flux on that flux coordinate. Such a bolometer radiation distribution is shown in Fig. 7(a) for a detached highly radiating plasma.

The bolometer inversion used for Fig. 7(a) is constrained not to allow radiation on any flux surface at normalized poloidal flux greater than 1.06. However, we see the radiation is peaked well inside that location, so that the conclusion about which flux surfaces suffer radiation is unaffected.

The bolometer array has a limited number of spatial chords, so that the spatial resolution is limited, particularly compared to the SOL width. The tangential TV diagnostic provides CIII radiation data which is inverted using the assumption of toroidal symmetry to give 2-D poloidal profiles [8]. This 2-D profile was transformed to L_{pol} and normalized poloidal flux coordinates in the same way as the bolometer inversion, and plotted in Fig. 7(b). Although the camera is not absolutely calibrated, each of the many pixels of the camera provides a viewing chord through the plasma, so the spatial resolution is better than that of the bolometer array. The CIII emission data from the tangential TV has a spatial distribution similar to that of CIV, which accounts for

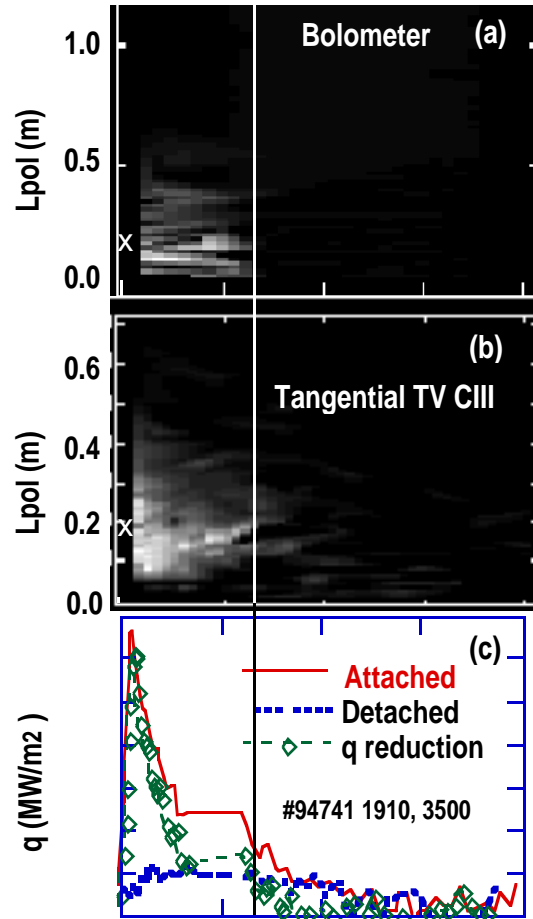


Fig. 7. (a) Radiation emissivity from outer SOL versus L_{pol} and normalized poloidal flux for bolometer for discharge 94741 at 3.5 s (detached) and (b) CIII radiation measured by tangential TV for discharge 94741 at 3.8 s (detached). The plasma changes little between 3.5 s and 3.8 s. The X-point is at $L_{pol} = 0.18$ m., normalized poloidal flux = 1, denoted by an X. (c) Divertor heat flux for a discharge mapped to normalized poloidal flux coordinates, for time slices before and during detachment, and the difference (q reduction). The vertical bar through all three plots is a guide for comparing heat flux with radiation at the same value of normalized poloidal flux. The horizontal scale is the same for 7(a), (b) and (c).

70%–80% of the power radiated near the X-point [9]. Therefore the tangential TV measures at higher resolution than bolometers the spatial distribution of radiated power near the X-point.

In Fig. 7(c) is shown an initial attached heat flux profile and the final detached profile for a discharge, plotted against normalized poloidal flux coordinates. Also shown in Fig. 7(c) is the difference (the diamonds joined by a thin dashed line) between the attached and detached profiles, indicating the heat flux which must have been removed upstream.

By comparing Fig. 7(a) and Fig. 7(c), we see that indeed the heat flux at the plate is reduced on flux surfaces on which there is upstream radiation (normalized poloidal flux < 1.07). There is heat flowing on flux surfaces farther out, as shown in both the initial and final profiles in

Fig. 7(a), but this heat flux reaches the plate undiminished because there is no significant radiation along the way. This conclusion is verified by comparing the tangential TV data in Fig. 7(b) with the heat flux in Fig. 7(c).

3. CONCLUSIONS

We have found the radiated power is linear with input power in both attached and detached plasma, with differing slopes. The linear dependence in the detached case is at least partially due to increased gas puffing at higher power in the experiments studied. The fraction of input power radiated is roughly constant at 0.7 as a function of input power for our highest power detached discharges.

The total divertor plate power for attached plasma is linear with input power as expected, as is \hat{q} . The detached total divertor power is also linear with input power, but \hat{q} saturates at approximately 1.2 MW/m². This difference in the dependence on input power is a result of the changes in profile shape when the heat flux at the strike point is dissipated in the PDD, and radiant heating increases over the whole divertor plate profile. If this saturation of detached heat flux occurs in larger machines at higher input power levels, it will be quite beneficial.

The radiant heating of the divertor plate increases linearly with input power. On average, half of the divertor plate power in a PDD plasma is due to absorbed radiation and half due to particles.

Comparison of the heat flux and radiation shows that the flux surfaces on which plate heating is reduced in the PDD are the same flux surfaces on which radiation is emitted upstream.

REFERENCES

- [1] A.W. Leonard, M.A. Mahdavi, S.L. Allen, *et al.*, Phys. Rev. Lett. **78** (1997) 4769.
- [2] T.W. Petrie, D.N. Hill, S.L. Allen, *et al.*, Nucl. Fusion **37** (1997) 321–338.
- [3] D.N. Hill, A. Futch, A.W. Leonard, *et al.*, J. Nucl. Mater. **196–198** (1992) 204–209.
- [4] C.J. Lasnier, D.N. Hill, T.W. Petrie, *et al.*, “Survey of target plate heat flux in diverted DIII–D tokamak discharges,” to be published in Nucl. Fusion
- [5] A.W. Leonard, C.J. Lasnier, J.W. Cuthbertson, *et al.*, J. Nucl. Mater. **220–222** (1995) 325.
- [6] A.W. Leonard, S.L. Allen, M.E. Fenstermacher, *et al.*, Proc. of the 22nd Euro. Conf. on Contr. Fusion and Plasma Physics European Physical Society, Petit-Lancy, Switzerland, Bournemouth, UK, 1995, **3**, 105.
- [7] A.W. Leonard, G.D. Porter, R.D. Wood, *et al.*, Phys. Plasmas **5** (1998) 1736.
- [8] M.E. Fenstermacher, W.H. Meyer, R.D. Wood, *et al.*, Rev. Sci. Instrum. **68** (1997) 974.
- [9] M. E. Fenstermacher *et al.*, Phys. Plasmas **4** (1997) 1761.

ACKNOWLEDGMENTS

Work supported by U.S. Department of Energy under Contract Nos. DE-AC03-89ER51114, W-7405-ENG-48, and DE-AC04-94AL85000.